Low Power Consumption (< 1 W) Mid-Infrared Quantum Cascade Laser for Gas Sensing

Hiroyuki YOSHINAGA*, Hiroki MORI, Jun-ichi HASHIMOTO, Yukihiro TSUJI, Makoto MURATA and Tsukuru KATSUYAMA

Quantum cascade lasers (QCLs) are promising compact light sources for high-speed and high-sensitivity gas sensing in the mid-infrared region. A QCL has high-speed performance, and its lasing wavelength can cover the entire mid-infrared region by controlling the thickness and composition of the superlattice layers in the active region. For the practical use of QCLs, their power-consumption needs to be reduced to 1 W or lower. However, as reducing the operation voltage of a QCL is difficult due to its oscillation mechanism, the threshold current needs to be reduced to reduce power consumption. For this purpose, we reduced the size of a QCL by adopting a buried hetero structure, high-reflectivity facet coating, and our original vertical transition active layer. As a result, we reduced the threshold current and succeeded in developing a low power-consumption QCL with a threshold power consumption as low as 0.52 W under continuous wave (CW) operation at 27˚C.

Keywords: quantum cascade laser, QCL, mid-infrared, gas-sensing, low power-consumption

1. Introduction

The mid-infrared (MIR) wavelength region (3 μm-20 μm) has attracted much attention as a most promising area for gas-sensing because absorption lines of various kinds of major industrial and environmental gases, such as CO_2, NO_x, and SO_x, exist there. The absorptions of the gases in the MIR region are mainly due to fundamental vibrational resonances of the molecules, which are several orders of magnitude larger than those due to higher-order harmonics in the near infrared (NIR) region[1]. Therefore, high-sensitive gas sensors can be realized easily in the MIR region, and demands for them will rapidly increase with the progress of their application in fields such as industrial and environmental gas measurements, medical diagnosis, and home security.

In future gas-sensings, measurements outdoors or short-time measurements in the case of the breath analysis and so on will be necessary, so gas sensors will need to be compact and high-speed. In addition, cost-reduction will also be essential for them to be used broadly. Considering the above requirements, semiconductor lasers are the best candidate for light sources of gas sensors because they are very small, high-speed, and their costs can be reduced sufficiently in mass-production using large-scale semiconductor substrates.

However, conventional semiconductor lasers based on a pn-junction have difficulty in lasing in the MIR region because the bandgaps, determined by the pn-junction, do not cover that wavelength region. To overcome this problem, a novel semiconductor laser, namely, a quantum cascade laser (QCL), in which a new-type emission region called core region was adopted for oscillation in the MIR region, was invented in 1994[2].

Figure 1 is a schematic diagram showing an example of a core region structure of a QCL. As shown, the core structure consists of several tens of unit structures stacked on one another. Each unit structure has an active region serving as a light-emitting region and an injector region to inject carriers (electrons) into the active region which both are made of super-lattice structures.
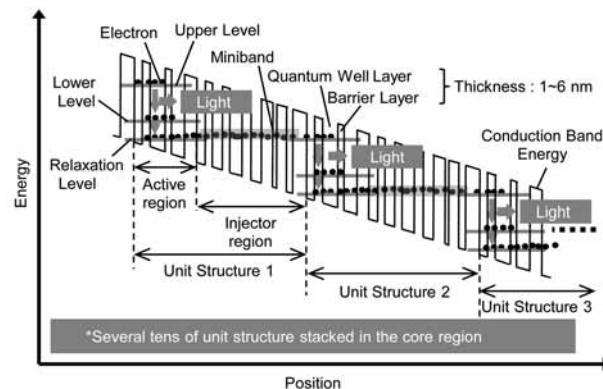
Fig. 1. Example of core region structure.

In QCLs, as shown in this figure, the radiative transitions between the sub-bands of the conduction band of the active region and subsequent carrier transportations to the next active regions through the mini-bands of the injector regions by tunneling effect make it possible to oscillate in the MIR wavelength region. They can lase in the entire MIR wavelength region by adjusting material compositions and thicknesses of the super-lattice layers in the active region. In addition, they have high relaxation oscillation frequencies, and high-speed characteristics.

After the first successful operation of the QCL in 1994[2], much technical progress was made, leading to characteristic improvements, such as a continuous-wave (CW) operation at room temperature (RT)[3]-[6], and an output-power increase up to several W[7], [8]. Distributed feedback

(DFB) QCLs with single-mode property have also been developed as a suitable light source for a gas sensor because a single-mode operation is desirable for detecting the particular absorption line of the target gas[9]-[12].

2. Motivation

In order to improve the QCL characteristics, it is important to increase the carrier transition probability between the sub-bands as well as to reduce the optical loss due to the non-radiative recombination caused predominantly by longitudinal optical phonon (LO phonon) scattering. To address this issue, we have developed our original vertical-transition active region structure[13]; in which high optical gain can be expected due to the vertical-transition of carriers between the sub-bands in the conduction band of the same quantum well in the active region while suppressing the LO-phonon scattering.

On the other hand, for the application of QCLs to gas-sensors used outdoors, they should be operated under CW condition at RT, and their power consumptions should be reduced sufficiently (< 1W) to make operation by a battery possible.

However, because high operation voltages (6-10 V) are inevitable, in principle, for QCL oscillation, a threshold current decrease is essential to realize a low power-consumption below 1 W. For this threshold current decrease, it is important to adopt an active region with high optical gain and a device structure in which internal losses due to absorption, scattering and so on are small, and high heat dissipation from the core region can be possible. High-reflective (HR) facets to reduce the cavity loss are also necessary for this purpose.

Based on these considerations, we introduced the above-mentioned vertical-transition active region structure with high gain into the core region of the QCL. As for the device structure, we first used a double channel (DC) structure[14], in which etched side walls of a mesa-waveguide were covered with dielectric insulating films for current confinement. This structure was easy to fabricate, but it was inadequate for threshold current reduction because of its low heat dissipation and high internal loss. Hence we replaced it with a buried-hetero (BH) structure, in which both sides of a mesa-waveguide were buried with a semi-insulating InP current blocking layers. It has a high heat dissipation and small internal loss due to the semi-insulating InP current blocking layer with high thermal conductivity and low optical loss, which is favorable for threshold current reduction. Finally, we applied HR facet coatings using Au to reduce the cavity-loss significantly. Combining these improvements, we reduced the threshold current of our QCL, and thus lowered its power-consumption.

3. Fabrication

The epitaxial growth was done by organometallic vapor phase epitaxy (OMVPE). In the first growth, a core region, a n-InP cladding layer, and an n-GaInAs contact layer were successively grown on an n-InP substrate. Then, the wafer was processed into a 10 μm wide mesa-stripe waveguide using photolithography and dry-etching, and was buried by an Fe-doped InP current-blocking layer in the second growth to form a BH structure. The core region consisted of 33 stages of unit structure containing active/injector regions constructed by AlInAs/GaInAs superlattices, and the active region had the vertical-transition structure mentioned above.

After forming the BH structure, an insulating film was deposited on the entire wafer. Then, the insulating film on the n-GaInAs contact layer was selectively removed by etching, and an ohmic electrode was formed there by evaporation. After adding a thick Au plating layer on the electrode, the substrate was thinned by grinding to the extent that laser bars could be easily made from the wafer by cleaving. Then, an electrode was formed on the back surface of the substrate, and thus our QCL was completed. Finally, laser bars were made by cleavage, and HR facet coatings using Au were applied to both facets of them.

Here, to prevent short-circuit at the facets caused by the Au coating, a highly-resistive alumina film was inserted between the Au film and the facet. The reflectivity of the rear facet need to be as high as possible to reduce the threshold current effectively, so the Au thickness of the rear facet was made to be large enough to obtain high reflectivity, around 100%. On the other hand, the reflectivity of the front facet was made to be intermediately high, around 70%, to extract an optical output from the front facet, and we, therefore, adopted a thin Au coating film as explained below.

Furthermore, we fabricated DC-QCLs as a reference to be compared with the BH-QCLs. Both QCLs had the same structure except for the current blocking region. We also used the DC-QCL in the Au coating experiment, as described in the next section, because its easy fabrication made it possible to complete the experiment in a short period of time.

4. Results and Discussions

4-1 HR facet coating experiments

Figure 2 shows the calculation result on the reflectivity of the Au-coated facet with the Au thickness as a parameter. As shown in this figure, it reaches to the highest reflectivity, around total reflection of 100%, with the Au thickness being more than about 50 nm, and then it saturates. Based on this calculation, an Au thickness of 100 nm would be sufficient to obtain a facet reflectivity near 100%, and we, therefore, adopted this thickness for the rear facet coating. In fact, we confirmed experimentally that the rear facet had a high reflectivity of nearly 100% with this Au thickness.

As for the front facet, it is known from **Fig. 2** that the Au thickness should be as thin as 5 nm or less to control the facet reflectivity to be the desired value of around 70%. However, as shown in this figure, the facet reflectivity changes sensitively with the Au thickness fluctuation in this
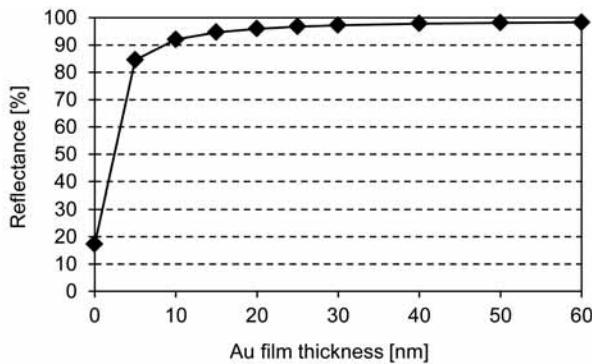
Fig. 2. Calculation result of Au-coated facet reflectivity with Au thickness as a parameter

reflectivity region. To cope with this issue, we optimized the Au coating condition to realize a precise control of the Au thickness.

We then performed Au coating experiments, using DC-QCLs having 0.5, 1, and 2 mm cavity lengths, to confirm the threshold current decrease by this coating. In these experiments, the Au thicknesses of the front and the rear facets were set to be of the values which could achieve 70% and 100% reflectivities, respectively. We measured the threshold currents of the above QCLs under pulsed condition at RT.

Figure 3 shows calculated relationships between the reflectivity of the front facet and the threshold current at RT for the three different cavities. This calculation was performed based on the measured values of the internal loss and the optical gain of the QCL and the reflectivity of the rear facet which was assumed to be 100%. The measured threshold currents for QCLs with these cavity lengths are also shown in this figure for comparison. As shown, the calculated threshold current of each cavity length decreases with the increase of the front facet reflectivity, and they are all coincide with the measured values at around 70%, which demonstrates that the actual reflectivity of the front facet was around 70%, as we aimed at.

4-2 Characteristics improvements by BH-structure

In the QCL measurements, we first investigated the characteristics improvements by replacing the DC-structure with the BH-structure. **Figure 4** represents the threshold current dependence on mesa-stripe width for both types of QCLs under pulsed condition at RT. All the measured chips were 3 mm long, and uncoated. As shown, while the DC-QCL could not lase with the mesa-width below 7 µm, the BH-QCL could lase even with the mesa-width as narrow as 5 µm and the threshold current at this mesa-width was significantly smaller than that of the DC-QCL at 7 µm mesa-width. From this result, it is clear that the introduction of the BH-structure is effective in reducing the threshold current, as we expected. The successful oscillation of BH-QCL in the narrow stripe-width region would be due to the reduction of internal loss caused by replacing the DC-structure with the BH structure.
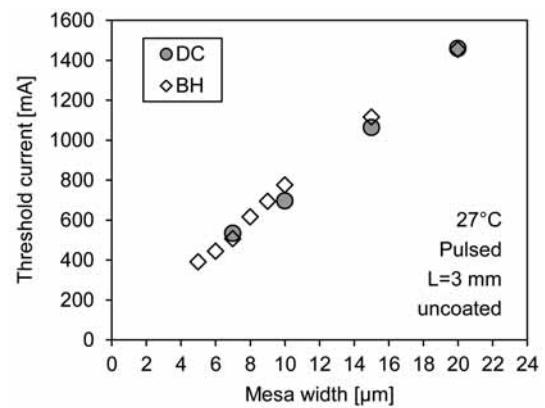
Fig. 4. Threshold current dependence on mesa-width

Next, we evaluated a thermal resistance reduction by introducing the BH-structure. **Figure 5** shows a comparison of the thermal resistance between the DC-QCL and BH-QCL uncoated chips, which both had a 3-mm long cavity length and a 10 µm wide mesa-stripe width. The thermal

Fig. 3. Relationship between the threshold current and front facet reflectivity
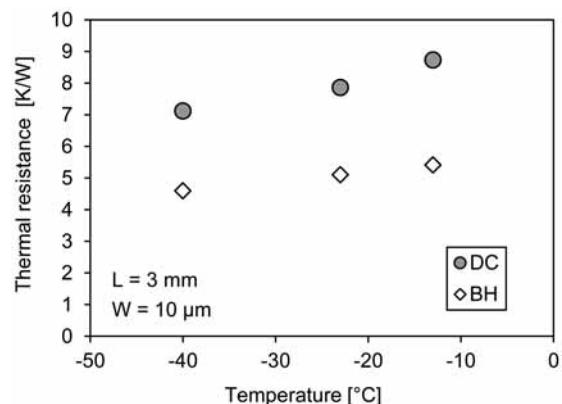
Fig. 5. Comparison of thermal resistance.

resistance was estimated from the threshold current difference between them under pulsed and CW conditions. The thermal resistances of the BH-QCL were found to be about 35% lower than those of the DC-QCL at every temperature, which demonstrates that the heat dissipation from the core region is significantly increased by changing the current blocking layer from the dielectric insulating film in DC-QCL to the semi-insulating InP in BH-QCL. Therefore, in comparison with the DC-QCLs, lower CW threshold currents are expected for BH-QCL, due to its excellent heat dissipation.

4-3 Power-consumption reduction in BH-QCL

We next investigated how much the threshold current of the BH-QCL could be reduced by shortening the cavity length, narrowing the mesa-stripe width, and applying an HR facet coating. **Figure 6** shows I-L characteristics of the HR coated BH-QCL, which had the shortest cavity-length of 0.5 mm and the narrowest mesa-stripe width of 5 μm, mounted on heatsinks in an epi-side down configuration.

The smallest threshold current was obtained in this QCL. By adopting the BH-structure with a low internal loss and a high thermal conductivity and applying the HR facet coating for reducing cavity loss, the considerable down-sizing of QCL chip mentioned above was possible, leading to this very low threshold current. As shown in this figure, the threshold current of the BH-QCL under a pulsed condition at 27°C was 57.4 mA, which had been remarkably reduced compared with the minimum threshold current of 130 mA in the conventional DC-QCL.

Furthermore, while a CW oscillation at 27°C was difficult in the DC-QCL, it was possible in the BH-QCL with the threshold current of 65 mA due to its narrower stripe width and a higher thermal conductivity as shown in **Fig. 6**. We also confirmed from the results of **Fig. 6** that the threshold power-consumptions at 27°C were 0.42 W and 0.52 W for the pulsed and CW conditions, respectively, and thus we succeeded in realizing a QCL with low power-consumption (< 1W).
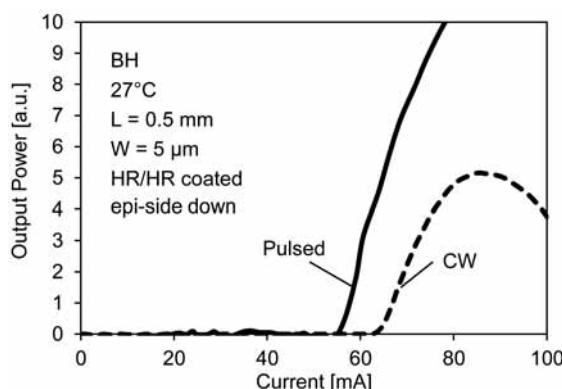
Fig. 6. I-L characteristics of BH-QCL.

Finally, a lasing spectrum was measured for a BH-QCL with a 0.5 mm cavity-length and a 5 μm mesa-stripe width

under CW condition at 27°C. The result is shown in **Fig. 7**. This measurement was carried out using FTIR, and the wavenumber resolution and driving current were 0.2 cm^{-1} and 87 mA, respectively. The peak lasing wavelength was 7.41 μm, and it could be changed with injection current and device temperature. CH_4 and H_2S are among the main target gases for the gas-sensing in this wavelength region. For the gas-sensing application, a DFB-QCL with single-mode oscillation is desirable as previously mentioned, and therefore, in the next stage, we will develop this type-of QCL based on the BH-device structure developed in this study.
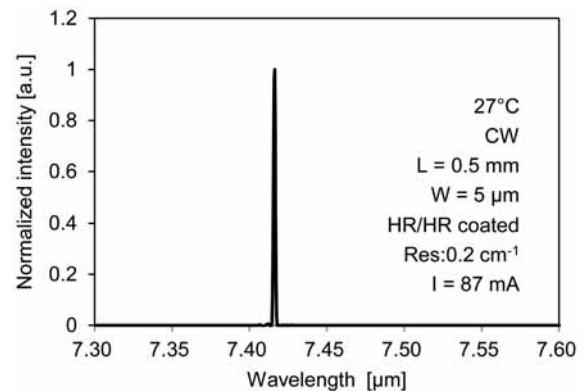
Fig. 7. Lasing spectrum of BH-QCL.

5. Conclusion

We developed a low-power consumption MIR-QCL for the gas-sensing application. For realizing a low power-consumption by reducing a threshold current, we adopted our original vertical-transition active region, a BH-structure with a low internal loss and a high thermal conductivity, and an HR facet coating using Au film. As a result, we succeeded in developing a low power-consumption QCL having a threshold power-consumption of 0.52 W under CW condition at 27°C. Development of a DFB-QCL with a single-mode operation for gas-sensing is the next issue to be treated in future work.

References

(1) Mid-IR Lasers Market Review and Forecast 2010, Strategies unlimited (2010)

(2) J. Faist, F. Capasso, D. L. Sivco, C. Sirtori, A. L. Hutchinson, A. Y. Cho, "Quantum Cascade Laser," Science, vol. 264, no. 5158, pp. 553-556 (1994)

(3) M. Beck, D. Hofstetter, T. Aellen, J. Faist, U. Oesterle, M. Ilegems, E. Gini, H. Melchior, "Continuous Wave Operation of a Mid-Infrared Semiconductor Laser at Room Temperature," Science, vol. 295, no. 5553, pp. 301-305 (2002)

(4) J. S. Yu, S. Slivken, A. Evans, L. Doris and M. Razeghi, "High-power continuous-wave operation of a 6 μm quantum-cascade laser at room temperature," Appl. Phys. Lett., vol. 83, 2503 (2003)

(5) M. Troccoli, S. Corzine, D. Bour, J. Zhu, O. Assayag, L. Diehl, B. G. Lee, G. Höfler and F. Capasso, "Room temperature continuous-wave operation of quantum-cascade lasers grown by metal organic vapor phase epitaxy," Electron. Lett., vol. 41, No. 19, pp. 1059-1060 (2005)

(6) K. Fujita, S. Furuta, A. Sugiyama, T. Ochiai, T. Edamura, N. Akikusa, M. Yamanishi, and H. Kan, "Room temperature, continuous-wave operation of quantum cascade lasers with single phonon resonance-continuum depopulation structures grown by metal organic vapor-phase epitaxy," Appl. Phys. Lett., vol. 91, 141121 (2007)

(7) Y. Bai, S. R. Darvish, S. Slivken, W. Zhang, A. Evans, J. Nguyen, and M. Razeghi, "Room temperature continuous wave operation of quantum cascade lasers with watt-level optical power," Appl. Phys. Lett., vol. 92, 101105 (2008)

(8) Y. Bai, S. Slivken, S. R. Darvish, and M. Razeghi, "Room temperature continuous wave operation of quantum cascade lasers with 12.5% wall plug efficiency," Appl. Phys. Lett., vol. 93, 021103 (2008)

(9) J. Faist, C. Gmachl, F. Capasso, C. Sirtori, D. L. Sivco, J. N. Baillargeon, and A. Y. Cho, "Distributed feedback quantum cascade lasers," Appl. Phys. Lett., vol. 70, 2670 (1997)

(10) S. Blaser, D. A. Yarekha, L. Hvozdara, Y. Bonetti, A. Muller, M. Giovannini and J. Faist, "Room-temperature, continuous-wave, single-mode quantum-cascade lasers at λ≈5.4 μm," Appl. Phys. Lett., vol. 86, 041109 (2005)

(11) J. S. Yu, S. Slivken, S. R. Darvish, A. Evans, B. Gokden, and M. Razeghi, "High-power, room- temperature, and continuous-wave operation of distributed-feedback quantum-cascade lasers at λ~4.8 μm," Appl. Phys. Lett., vol. 87, 041104 (2005)

(12) Tadataka Edamura, Naota Akikusa, Atsushi Sugiyama, Takahide Ochiai, Masamichi Yamanishi, Kiyoji Uehara, and Hirofumi Kan, "Single-mode distributed-feedback quantum cascade laser for high sensitivity gas spectroscopy," IEICE Technical Report, vol. 105, LQE2005-119, pp. 29-32 (2005)

(13) Jun-ichi Hashimoto, Yukihiro Tsuji, Hiroshi Inada, Makoto Murata, Hiroyuki Yoshinaga, Hideki Yagi, Takashi Kato, Michio Murata, and Tsukuru Katsuyama, "Mid-IR vertical transition DFB quantum cascade laser," IEICE Technical Report, vol. 111, LQE2011-152, pp. 109-113 (2012)

(14) J. S. Yu, S. Slivken, A. Evans, J. David, and M. Razeghi, "Very high average power at room temperature from λ≈5.9-μm quantum-cascade lasers," Appl. Phys. Lett., vol. 82, 3397 (2003)

~~~~~~

Contributors (The lead author is indicated by an asterisk (∗).)

H. YOSHINAGA*
• Assistant Manager, Transmission Devices R&D Laboratories

H. MORI
• Assistant Manager, Transmission Devices R&D Laboratories

J. HASHIMOTO
• Dr. Eng.
  Group Manager, Transmission Devices R&D Laboratories

Y. TSUJI
• Assistant Manager, Transmission Devices R&D Laboratories

M. MURATA
• Dr. Sci.
  Transmission Devices R&D Laboratories

T. KATSUYAMA
• Senior Specialist, Dr. Eng.
  Department Manager, Transmission Devices R&D Laboratories